

Searching for particle-hole cluster bands in ^{8}Be using the ISOLDE Solenoidal Spectrometer

HAVERSON, Kristian CZ, SMITH, Robin <<http://orcid.org/0000-0002-9671-8599>>, GAI, Moshe, HUGHES, Owen, TINDLE, Olivia, BISHOP, Jack, BROOKS, Alexander D, FALEZZA, Filippo, KOKALOVA, Tzany, PIRRIE, Stuart, STAJKOWSKI, Dominik, WHELDON, Carl, BUTLER, Peter A, DOLAN, Annie, GAFFNEY, Liam P, JONES, Ben, OJALA, Joonas, ROWNTREE, Faye, SHARP, David K, REEVE, Samuel, FREEMAN, Sean J, MACGREGOR, Patrick T, LABICHE, Marc, GOMEZ-RAMOS, Mario, CASAL, Jesus and AL-AQEEL, Muneerah AM

Available from Sheffield Hallam University Research Archive (SHURA) at:

<https://shura.shu.ac.uk/34605/>

This document is the Published Version [VoR]

Citation:

HAVERSON, Kristian CZ, SMITH, Robin, GAI, Moshe, HUGHES, Owen, TINDLE, Olivia, BISHOP, Jack, BROOKS, Alexander D, FALEZZA, Filippo, KOKALOVA, Tzany, PIRRIE, Stuart, STAJKOWSKI, Dominik, WHELDON, Carl, BUTLER, Peter A, DOLAN, Annie, GAFFNEY, Liam P, JONES, Ben, OJALA, Joonas, ROWNTREE, Faye, SHARP, David K, REEVE, Samuel, FREEMAN, Sean J, MACGREGOR, Patrick T, LABICHE, Marc, GOMEZ-RAMOS, Mario, CASAL, Jesus and AL-AQEEL, Muneerah AM (2024). Searching for particle-hole cluster bands in ^{8}Be using the ISOLDE Solenoidal Spectrometer. EPJ Web of Conferences, 311: 00012. [Article]

Copyright and re-use policy

See <http://shura.shu.ac.uk/information.html>

Searching for particle-hole cluster bands in ^8Be using the ISOLDE Solenoidal Spectrometer

Kristian C. Z. Haverson^{1,*}, Robin Smith^{1,2,**}, Moshe Gai², Owen Hughes¹, Olivia Tindle¹, Jack Bishop³, Alexander D. Brooks³, Filippo Falezza³, Tzany Kokalova³, Stuart Pirrie³, Dominik Stajkowski³, Carl Wheldon³, Peter A. Butler⁴, Annie Dolan⁴, Liam P. Gaffney⁴, Ben Jones⁴, Joonas Ojala⁴, Faye Rowntree⁴, David K. Sharp⁵, Samuel Reeve⁵, Sean J. Freeman⁵, Patrick T. MacGregor⁶, Marc Labiche⁷, Mario Gomez-Ramos⁸, Jesus Casal⁸, and Muneerah A. M. Al-Aqeel⁹

¹Materials and Engineering Research Institute, Sheffield Hallam University, Sheffield, UK

²Laboratory for Nuclear Science, University of Connecticut, Groton, CT 06340, USA

³School of Physics and Astronomy, University of Birmingham, Birmingham, B15 2TT, UK

⁴Oliver Lodge Laboratory, University of Liverpool, Liverpool L69 7ZE, UK

⁵Department of Physics, University of Manchester, Manchester, M13 9PL, UK

⁶CERN, Geneva 23 CH-1211, Switzerland

⁷Nuclear Physics Group, UKRI-STFC Daresbury Laboratory, Daresbury, WA4 4AD, UK

⁸Departamento de Física Atómica, Molecular y Nuclear, Universidad de Sevilla, Spain

⁹College of Science Imam Mohammad Ibn Saud Islamic University Riyadh, Saudi Arabia

Abstract. The $^7\text{Be}(d, p)^8\text{Be}^*$ reaction was measured in inverse kinematics at a beam energy of 11 MeV/u using the ISOLDE Solenoidal Spectrometer, in order to identify and characterise high-excitation states in ^8Be . The spin-parities of many of the states in the 16–20 MeV region can be explained as being particle-hole excitations within a two-centre shell model. The present experiment aims to elucidate the spin parities of higher excited states, > 20 MeV, to assess their candidacy as rotational excitations of the aforementioned particle-hole states. The beam intensity in this experiment was measured using a downstream Micron S1 double-sided silicon strip detector to pick up elastically scattered deuterons. The focus of this paper is to present methods for calculating the beam intensity, which is key for extracting the spectroscopic factors of the measured states. Preliminary excitation spectra are also presented.

1 Introduction

Clues to the underlying α -cluster structure of ^8Be have been present ever since the very first accelerator-induced nuclear reactions were measured by Cockroft and Walton [1]. In their seminal paper, *Disintegration of Lithium by Swift Protons*, they observed the capture of a proton by lithium-7, producing two α particles. Since then, the 2α structure of ^8Be has become well-established; the rotational band, with 2^+ and 4^+ members at 3.03 and 11.35 MeV, built upon the short-lived ground state, possesses a large moment of inertia commensurate with a dumbbell-like 2α structure.

*e-mail: k.haverson@shu.ac.uk

**e-mail: robin.smith@shu.ac.uk

There are several different approaches to describing this nucleus from a theoretical perspective. In one corner, there are the Algebraic Cluster Model (ACM) calculations of Bijker and Iachello [2], which apply geometrical point group symmetries to nuclear states, where the α clustering is built explicitly into the theory. In another corner, there are computationally-intensive *ab-initio* approaches such as the No-Core Shell Model [3, 4] and Green's Function Monte Carlo [5], which can readily be applied to these light nuclei, and where clustering is seen to emerge naturally from the underlying nucleon-nucleon interaction. In the third corner is the α condensate model. The possibility of α -particle condensation in infinite matter was originally found to be possible at low densities (below a fifth of the nuclear saturation density) [6]. The case of finite nuclear systems was first approached in a flagship paper by Tohsaki, Horiuchi, Schuck and Röpke (THSR) [7], who concluded that such a condensate state could exist in light α -conjugate nuclei at energies around the α -decay threshold, like the ground state of ^8Be .

The α particle is a particularly sturdy structure, with an exceptionally tight binding energy of 28.3 MeV. Hence, the preferred preformation as a cluster in the nucleus is hardly surprising. However, as the excitation energy of an α -clustered nucleus increases, and the α particle becomes a less stable building block, the structure of the nucleus may change. Helium-4 has an excited 0^+ state at 20.2 MeV which corresponds to a $1p-1h$ excitation to the *sd*-shell, and previous experimental work has found evidence for states between 23–25 MeV in ^8Be , which decay through the excited ^4He [8]. This indicates a shift away from the simple 2α structure seen for the ground state rotational band.

The known higher energy parts of the ^8Be spectrum can be described phenomenologically using the Cluster Shell Model (CSM), which has been discussed previously by Gai [9, 10]. This model relies on the two-centre shell model [11–13], which calculates single-particle levels in a two-centre potential corresponding to two α particles. It has been shown that the states in ^8Be from 16–20 MeV can all be described as particle-hole (*p-h*) excitations within the CSM framework [10]. This phenomenological agreement serves as a motivation to consider measurements of the spectroscopy of ^8Be above 20 MeV [14, 15], where one might expect rotational excitations to exist built upon *p-h* cluster states.

The aim of the present experiment was to measure branching ratios and spectroscopic factors for known states in ^8Be with $E_x < 20$ MeV, and explore its spectroscopy above 20 MeV. In particular, confirmation of a possible 3^- assignment for the broad state at 21.5 MeV could indicate it belongs to a $K^\pi = 2^-$ rotational band built upon a *p-h* intrinsic state.

2 Experiment details

The experiment was conducted at the ISOLDE facility [16] at CERN in Geneva, where the $^7\text{Be}(d, p)^8\text{Be}^*$ reaction was measured in inverse kinematics. An 11.08 MeV/u ^7Be beam was produced by accelerating ions from a pre-irradiated target, using the Laser Ion Source (RILIS) [17]. The experiment was conducted with offline beam production to minimise ^7Li contamination in the beam. The beam was subsequently directed to the Electron Beam Ion Source (EBIS) charge breeder, where ^7Be ions were ionised to the 4^+ charge state and accelerated.

The beam was then transported to the target station contained within the ISOLDE Solenoidal Spectrometer (ISS) [18]. This set-up consists of a series of silicon charged particle detectors enclosed by a repurposed MRI magnet with a bore radius of 46.25 cm. Throughout the experiment, the magnet was maintained at a nominal field strength of 1.42 T. A rendering of the ISS configuration used in this experiment is shown in figure 1.

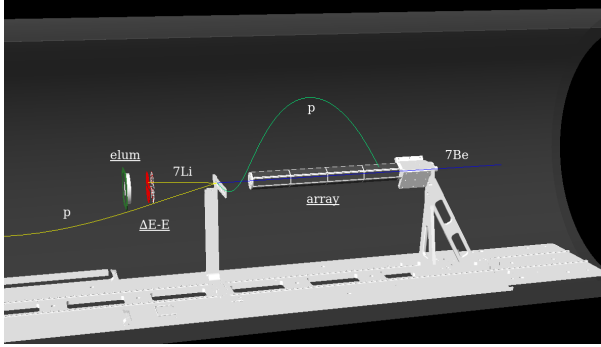


Figure 1. A rendering of the ISS and a typical reaction, generated using NPTool [19]. The ${}^7\text{Be}$ beam enters from right to left. The protons ejected at backward lab angles are detected by a hexagonal arrangement of silicon detectors upstream of the target that surround the beam. The decay products of the ${}^8\text{Be}$ are detected by a downstream $\Delta E - E$ telescope. The beam intensity is measured by a shielded beam monitoring silicon detector further downstream.

For this experiment, two targets were used: a $240 \mu\text{g}/\text{cm}^2$ CD_2 (deuterated polyethylene) target and a $225 \mu\text{g}/\text{cm}^2$ ${}^{12}\text{C}$ target. The latter was specifically used for background estimation.

Beam intensity was monitored using an energy-sensitive luminosity detector “*elum*” positioned downstream 293 mm from the target ladder and centred on the beam axis. This is a Micron S1 silicon detector with a thickness of $297 \mu\text{m}$, an inner radius of 24 mm, and an outer radius of 48 mm. This detector was used to measure recoiling deuterons from ${}^7\text{Be}(d, d)$ elastic scattering. The deuterons had a very narrow angular range of acceptance, from 24.39 – 24.61 degrees θ_{cm} , due to a thick aluminium shield mounted 9 mm from the face of the luminosity detector.

For the ${}^7\text{Be}(d, p)$ reaction, ejected protons were detected at backward angles using the ISS on-axis proton array, which enabled the measurement of their energy and position. The array comprises three modules, each containing eight double-sided silicon strip detectors (DSSDs) arranged in four rows, with a total active length of 500 mm. The detectors are BB21 Micron silicon strip wafers. Each module is digitised, with four p-side (front strips) ASICs providing 128 physical channels each, and n-side (back strips) ASICs with 44 physical channels each, with additional channels reserved for pulser inputs. The signals undergo analogue shaping after the preamplifier on the front end of the ASICs, and a peak-hold circuit is used to measure the pulse height with a single ADC on each ASIC. Separate control logic is used to match the ADC events with the channel ID and timestamp before sending the data off the chip.

A downstream $\Delta E - E$ detector array was employed for recoil detection. Each layer of this array features four Micron QQQ1 detectors arranged in a circular geometry centred on the beam axis. The first ΔE layer was placed 206 mm from the target ladder, and there was a 14 mm gap between this and the second E layer. These detectors have an inner radius of 9 mm and an outer radius of 50 mm. The first layer of the detector is $69.5 \mu\text{m}$ thick, while the second layer is $502 \mu\text{m}$ thick. This configuration allowed excitation spectra to be gated on different decay channels of the recoiling ${}^8\text{Be}$, which included emission of α particles, ${}^7\text{Li}$, and ${}^7\text{Be}$. Data analysis was performed using the ISSort codebase [20].

3 Preliminary analysis

3.1 Beam intensity monitoring

The energy spectrum obtained from the *elum* luminosity monitor, was separated based on the time difference between the scattered beam detected in the ΔE layer of the recoil detector, and the measured signal in the *elum* detector, corresponding to the elastically scattered

deuteron from the target. The two prominent features in the left panel of figure 2 correspond to elastically scattered deuterons turning either once or twice in the magnetic field, before hitting the luminosity detector. The lower energy 2-turn events arrive later than the higher energy one-turn, as expected. The individual energy spectra corresponding to each class of event are shown in the right panel of figure 2.

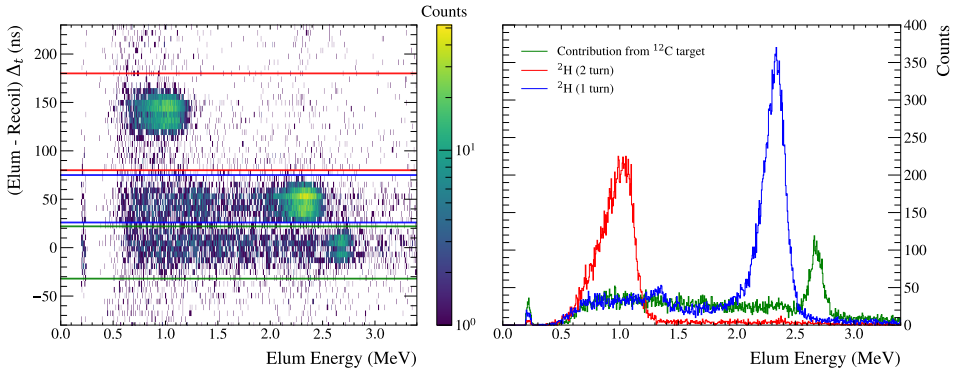


Figure 2. Left panel: the energy deposited in the luminosity detector vs. the time of arrival, measured relative to the recoil ΔE detector. Right panel: the luminosity detector energy spectra corresponding to different time cuts. The narrow green peak is thought to originate from reactions with the carbon in the target

The counts in the single turn deuteron spectra were obtained by fitting a skewed Gaussian plus a linear background term to the single turn peak. Then, Monte-Carlo simulations were used to generate an efficiency factor, ϵ , that accounted for geometric acceptance. This finite acceptance is due to deuterons hitting the bore of the solenoid or the detector mounting, and because not all events will result in a coincidence with the ΔE recoil detector. The simulation package used is called NPTool [19], which is an open source data analysis and Monte-Carlo simulation package for low-energy nuclear physics, which uses a GEANT4 and ROOT backend.

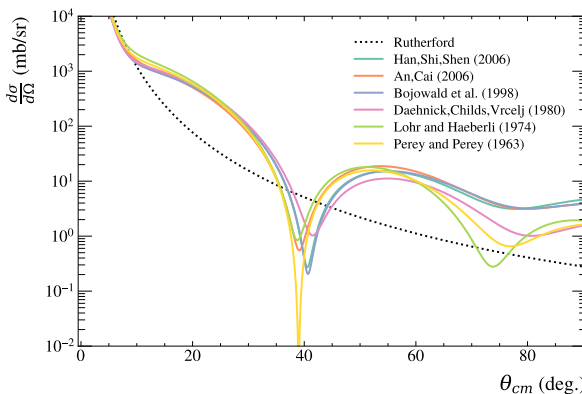


Figure 3. The differential cross sections for $^7Be(d, d)$ used in this analysis corresponding to the various optical model potentials. The Rutherford cross section is also drawn for comparison, which is in agreement at small scattering angles.

A number of optical model potentials were then calculated and used within Ptolemy to calculate elastic scattering differential cross sections for $^7Be(d, d)$ at the appropriate centre of

mass energy, as shown in figure 3. These were integrated over the solid angle coverage of the luminosity detector. The beam intensity, I , may then be calculated using the following formula:

$$I = \frac{Y/\epsilon}{Nt \int \frac{d\sigma}{d\Omega} d\Omega}, \quad (1)$$

where Y is the yield corresponding to the peak in the elum energy spectrum, ϵ is the efficiency, N is the number of target nuclei per unit area, t is the measurement time, and $d\sigma/d\Omega$ is the average of the differential cross sections calculated using Ptolemy. Future analyses will consider the two-turn deuteron peak and check for consistency.

3.2 Decay channel selection and excitation spectrum

As noted in section 2, detection of the protons in the backward angles allows high-resolution excitation spectra to be calculated, based on the position and energy of detected protons. Raw excitation spectra are polluted with contributions from events other than those originating from the desired ${}^7\text{Be}(d, p)$ reaction. Notably, protons and α particles from fusion evaporation reactions are likely a dominant background source. To combat this, decay products of the excited ${}^8\text{Be}$ are detected downstream in the $\Delta E - E$ telescope. A plot of ΔE vs. E permits the identification the detected particles, and hence a tag of the decay channel of the proposed excited ${}^8\text{Be}$, as shown in figure 4.

Further NPTool simulations were performed with the $\Delta E - E$ telescope and the ISS array included. The desired ${}^7\text{Be}(d, p)$ reaction was simulated in order to identify where on this plot recoils from the decay of ${}^8\text{Be}^*$ will lie. These Monte-Carlo events are overlaid onto the experimental data in figure 4. From here, software gates were placed, as shown by the black lines. Highlighted areas of the plot correspond to the detection of α particles, ${}^7\text{Li}$, and ${}^7\text{Be}$.

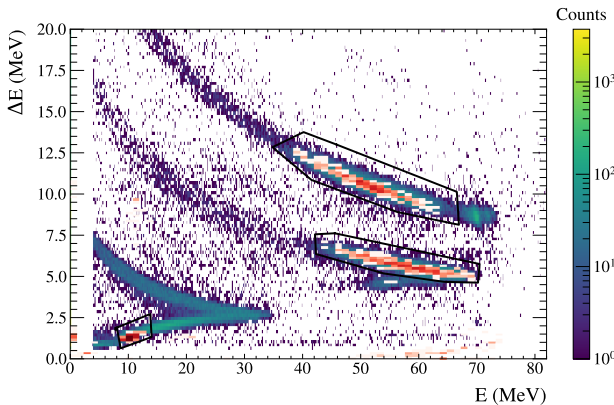


Figure 4. Experimentally measured (colour bar) and simulated $\Delta E - E$ (overlaid white-red colour) spectra. The use of simulation here is key, as there are large areas of the plot showing experimental data where they are not energetically allowed from the ${}^7\text{Be}(d, p)$ reaction under investigation. The main features, from bottom to top, correspond to detection of ${}^4\text{He}$, ${}^7\text{Li}$ and ${}^7\text{Be}$.

After gating on these three regions, preliminary excitation spectra were calculated, as shown in figure 5. The current spectra, although cleaned, still include some background from other reaction channels, along with events corresponding to interactions with the ${}^{12}\text{C}$ in the target. Additionally, more Monte-Carlo simulations are needed to accurately map out the efficiency of the array as a function of centre of mass angle and excitation energy to properly correct these spectra before angular distributions may be extracted.

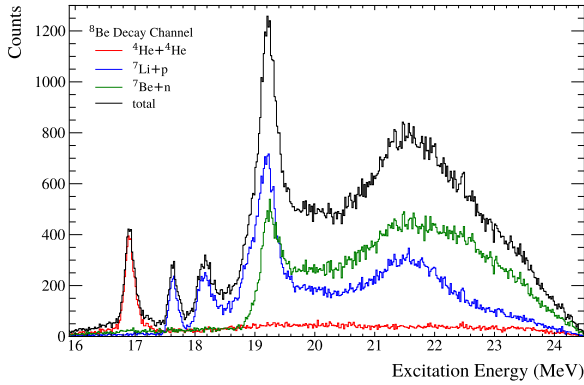


Figure 5. Preliminary excitation spectra corresponding to the main decay channels of ^8Be , as shown in figure 4. These spectra still require background subtraction and efficiency corrections.

4 Summary

The ISOLDE Solenoidal Spectrometer was used to measure the $^7\text{Be}(d, p)$ reaction in inverse kinematics. This paper presents preliminary particle identification plots and excitation spectra of ^8Be . It also presents the general method of measuring the beam intensity and some key analysis steps.

5 Acknowledgements

The authors would like to thank the staff of ISOLDE for providing high-quality beams during the experiments. This work is supported by the UK Science and Technology Facilities Council (STFC) (grant no's. ST/V001086/1 and ST/V001027/1). This project has received funding from the European Union's Horizon Europe Research and Innovation programme under Grant Agreement No. 101057511.

6 Rights retention statement

For the purpose of open access, the author has applied a Creative Commons Attribution (CC BY) licence to any Author Accepted Manuscript version arising from this submission.

References

- [1] J. D. Cockcroft, & E. T. S. Walton. *Nature*, 129(3261), 649-649 (1932).
- [2] R. Bijker and F. Iachello, *Ann. Phys.* 298, 334 (2002).
- [3] B. R. Barrett, P. Navrátil, & J. P. Vary. *Progress in Particle and Nuclear Physics*, 69, 131-181 (2013).
- [4] P. Maris, M. A. Caprio, & J. P. Vary. *Phys. Rev. C*, 91(1), 014310 (2015).
- [5] R. B. Wiringa, S. C. Pieper, J. Carlson & V. R. Pandharipande. *Phys. Rev. C* 62 014001 (2000).
- [6] G. Röpke, A. Schnell, P. Schuck, P. Nozières. *Phys. Rev. Lett.* 80, 3177 (1998).
- [7] A. Tohsaki, H. Horiuchi, P. Schuck, G. Röpke, Alpha cluster condensation in ^{12}C and ^{16}O . *Phys. Rev. Lett.* 87, 192501 (2001).

- [8] M. Freer et al. *J. Phys. G: Nucl. Part. Phys.* 35, 125108 (2008).
- [9] M. Gai. In *EPJ Web of Conferences* (Vol. 223, p. 01019). EDP Sciences (2019).
- [10] M. Gai. *Journal of Physics: Conference Series* (Vol. 2453, No. 1, p. 012024). IOP Publishing (2023).
- [11] D. Scharnweber, W. Greiner & U. Mosel. *Nucl. Phys. A* 164, pp. 257–278 (1971).
- [12] W. Z. von Oertzen *Phys. A Hadron Nucl.* 354, pp. 37–43. issn: 0939-7922 (1996).
- [13] V. Della Rocca, R. Bijker, & F. Iachello. *Nuclear Physics A*, 966, 158-184 (2017).
- [14] D. R. Tilley, J. H. Kelley, J. L. Godwin, D. J. Millener, J. Purcell, C. G. Sheu & H.R. Weller. *Nuclear Physics A*, 745(3-4), 155-362 (2004).
- [15] P. R. Page, *Phys. Rev. C* 72, 054312 (2005).
- [16] Y. Kadi, Y. Blumenfeld, R. Catherall, W. D. Venturini, M. J. G. Borge, M. Huyse, & P. V. Duppen. *HIE-ISOLDE: the future of Radioactive Beam Physics at CERN*. In *Challenges and Goals for Accelerators in the XXI Century* (pp. 585-610) (2021).
- [17] V. Fedosseev, K. Chrysalidis, T. D. Goodacre, B. Marsh, S. Rothe, C. Seiffert, and K. Wendt, *J. Phys. G: Nucl. Part. Phys.* 44, 084006 (2017).
- [18] <https://isolde-solenoidal-spectrometer.web.cern.ch/>
- [19] A. Matta et al., *J. Phys. G: Nucl.Part. Phys.* 43, 045113 (2016)
- [20] <https://doi.org/10.5281/zenodo.6366317>